The influence of the scaffold design on the distribution of adhering cells after perfusion cell seeding

Biomaterials 32 (2011) 2878–2884

Contents lists available at ScienceDirect

Biomaterials

journal homepage: www.elsevier.com/locate/biomaterials

The influence of the scaffold design on the distribution of adhering cells after perfusion cell seeding

Ferry P.W. Melchels [a,1], Beatrice Tonnarelli [b,1], Andy L. Olivares [c], Ivan Martin [b], Damien Lacroix [c], Jan Feijen [a], David J. Wendt [b], Dirk W. Grijpma [a,d,*]

[a] MIRA Institute for Biomedical Technology and Technical Medicine, Department of Polymer Chemistry and Biomaterials, University of Twente, P.O. Box 217, 7500 AE, Enschede, The Netherlands
[b] Departments of Surgery and of Biomedicine, University Hospital Basel, Hebelstrasse 20, 4031 Basel, Switzerland
[c] Institute for Bioengineering of Catalonia (IBEC), Baldiri Reixac 4, 08028 Barcelona, Spain
[d] Department of Biomedical Engineering, University Medical Centre Groningen and University of Groningen, P.O. Box 196, 9700 AD Groningen, The Netherlands

ARTICLE INFO

Article history:
Received 29 October 2010
Accepted 8 January 2011
Available online 1 February 2011

Keywords:
Scaffolds
Microstructure
Cell adhesion
Confocal microscopy
Image analysis
Computational fluid dynamics

ABSTRACT

In natural tissues, the extracellular matrix composition, cell density and physiological properties are often non-homogeneous. Here we describe a model system, in which the distribution of cells throughout tissue engineering scaffolds after perfusion seeding can be influenced by the pore architecture of the scaffold. Two scaffold types, both with gyroid pore architectures, were designed and built by stereolithography: one with isotropic pore size (412 ± 13 μm) and porosity (62 ± 1%), and another with a gradient in pore size (250–500 μm) and porosity (35%–85%). Computational fluid flow modelling showed a uniform distribution of flow velocities and wall shear rates (15–24 s^{-1}) for the isotropic architecture, and a gradient in the distribution of flow velocities and wall shear rates (12–38 s^{-1}) for the other architecture. The distribution of cells throughout perfusion-seeded scaffolds was visualised by confocal microscopy. The highest densities of cells correlated with regions of the scaffolds where the pores were larger, and the fluid velocities and wall shear rates were the highest. Under the applied perfusion conditions, cell deposition is mainly determined by local wall shear stress, which, in turn, is strongly influenced by the architecture of the pore network of the scaffold.

1. Introduction

Zonal variations in extracellular matrix composition, as well as in cell distribution, have been observed in native tissues like articular cartilage, meniscal- and osteochondral tissue. Tissue grafts engineered in vitro to possess anisotropic properties that mimic the complex in vivo organisation could lead to better tissue function, regeneration, and integration as compared to homogenous grafts.

Bi-zonal engineered tissues, with locally varying composition and structure, have been generated in bioreactors inducing hydrodynamic flow [1], however, little is known about the specific effects of fluid flow on cell behaviour. Computational models have been developed, based on micro-computed tomography (μCT) reconstructions of the scaffold pore networks, to assess the influence of the scaffold micro-architecture on local shear stress profiles within the scaffold pores [2]. However, the irregular and random pore structures of most 3D scaffolds present significant challenges when attempting to correlate computational data to experimental observations in specific regions of the scaffold. As an alternative, scaffolds fabricated by solid freeform fabrication techniques, such as stereolithography, can be produced to posses highly regular and well-defined pore architectures [3], allowing the establishment of relations between local field variables calculated for the fluid dynamic field and the cellular behaviour within the 3D construct as a function of spatial location.

It was previously demonstrated that the perfusion of a cell suspension directly through the pores of a scaffold with a random pore structure resulted in a highly uniform distribution of cells [4]. The initial homogeneous cell distribution established a template for spatially uniform extracellular matrix deposition during subsequent perfusion culture in the bioreactor system [5]. With the ultimate goal of engineering biomimetic zonal tissue grafts, in this work, we hypothesised that gradients in shear rate, induced by anisotropic gradient scaffold architectures, would modulate the cell distribution during perfusion cell seeding.

* Corresponding author. MIRA Institute for Biomedical Technology and Technical Medicine, and Department of Polymer Chemistry and Biomaterials, University of Twente, P.O. Box 217, 7500 AE, Enschede, The Netherlands. Tel.: +31 53 489 2966; fax: +31 53 489 2155.
E-mail address: d.w.grijpma@tnw.utwente.nl (D.W. Grijpma).
[1] Equally contributing authors.

0142-9612
doi:10.1016/j.biomaterials.2011.01.023

2. Experimental

2.1. Scaffolds

Photo-polymerisable poly(D,L-lactide) (PDLLA) macromers were synthesised in a similar way as previously described [6]. In short, linear hydroxy-terminated oligomers with a molecular weight of 1.2 kg/mol were synthesised by ring opening polymerisation, followed by a reaction for 9 h with methacrylic anhydride (Sigma–Aldrich, 50% molar excess) at 110 °C in the presence of 0.15% α-tocopherol inhibitor (vitamin E, Fluka) to prevent preliminary crosslinking. The excess methacrylic anhydride and the formed methacrylic acid were removed by vacuum distillation (residues 0.7 and 0.4 wt%, respectively). The macromers were used to formulate a stereolithography resin further comprising 18 wt% dry N-methylpyrrolidone (NMP, Fluka) as a non-reactive diluent, 3.6 wt% ethyl-2,4,6-trimethylbenzoylphenyl-phosphinate (Lucirin TPO-L photo-initiator from BASF) and 0.15 wt% Orasol Orange G dye (Ciba SC).

Two scaffold designs were developed using K3DSurf v0.6.2 software, both based on the gyroid architecture [3,6]. The first design is an isotropic design (type I) with constant porosity throughout the (cylindrical) scaffold. Another scaffold (type G) was designed to have a porosity gradient in the radial direction, by making the offset value in the implicit function (see below) dependent on the scaffold radius. The following equations were used to describe the scaffold designs, both with boundary conditions $x^2 + y^2 < (10\pi)^2$ and $|z| < 5\pi$:

$$I : \cos(x)\sin(y) + \cos(y)\sin(z) + \cos(z)\sin(x) - 0.15 = 0$$

$$G : \cos(x)\sin(y) + \cos(y)\sin(z) + \cos(z)\sin(x) + 0.0015\left(x^2 + y^2\right) - 0.90 = 0$$

Cylindrical scaffolds (diameter 8 mm, height 4 mm) were fabricated from CAD designs using an EnvisionTec Perfactory Mini Multilens stereolithography apparatus, and post-treated as previously described [6]. Micro computed tomography (μCT, GE eXplore Locus SP operated at 80 kV, 80 μA and 15 μm resolution without filter) was used for structural analyses of the fabricated scaffolds and to obtain digital meshes as input for flow analyses (MicroView software).

2.2. Fluid flow modelling

The flow of fluid (medium) through the pore networks of both scaffold types was modelled using a computational fluid dynamics approach, and taking the geometry of the bioreactor chamber into account. With μCT iso-surface meshes as input, volumetric fluid meshes were made using Mimics software (Materialise) to obtain a total of 2,375,010 tetrahedral elements for the type I scaffold and 2,253,778 elements for the type G scaffold. The boundary conditions used in modelling the perfusion were in correspondence with the perfusion cell seeding experiment (see below). No-slip surface conditions and zero outlet pressures were assumed. In the model, the material from which the scaffolds were prepared was rigid and impermeable. Profiles of fluid flow velocity, fluid shear rates and fluid shear stresses were calculated using Fluent 6.3 (Ansys) software. The fluid was modelled using the viscosity ($\eta = 1.45 \cdot 10^{-3}$ Pa·s) and density ($\rho = 1000$ kg·m^{-3}) of Dulbecco's modified eagle medium (DMEM, both at 37 °C).

2.3. Perfusion cell seeding

The scaffolds were perfusion seeded with expanded human articular chondrocytes (HAC) in separate bioreactors as previously described [4]. Scaffolds were lightly press-fit and clamped within a bioreactor chamber such that the fluid was forced to flow through its pores. Then, 3 million HAC suspended in 8 mL media per chamber were dynamically seeded for 16 h at an inlet velocity of 1 mm/s. Following perfusion seeding (3 specimens per scaffold architecture), cells were stained with SYTO-13 green fluorescent dye (Molecular Probes) to assess the distribution of live cells within the scaffolds. Confocal microscopy images were taken using a confocal laser scanning microscope (CLSM, 7500-Zeiss) with a 10× objective and the aperture set at 1 Airy unit (this corresponds to an image depth of 10 μm). Entire scaffold cross-sections were imaged by scanning over adjacent blocks of z-stacks, up to 500 μm in depth. The confocal microscopy images were thresholded to black-and-white and subsequently used to determine relative cell densities. Relative cell densities were expressed as the relative area of the image covered with cells (the fraction of black pixels). To obtain quantitative distributions as a function of the scaffold radius, the coordinates of each scaffold centre were first determined. The images were then partitioned in equidistant rings from the centre towards the periphery with radius increments of 100 μm. The cell density in each concentric ring was determined, as the percentage of the area covered with cells. The quantitative results of the cell distributions are averaged over at least 21 confocal images per each analysed sample.

The polar moments of inertia for wall shear rate and cell density were calculated using:

$$J = \iint r^2 \rho(\vec{r}) dA = \sum_i^N r_i^2 \rho_i \pi \left(r_i^2 - r_{i-1}^2\right)$$

where r is the distance from the scaffold centre, ρ is the density function of either the local average wall shear rate or the cell density, and $dA = \pi(r_i^2 - r_{i-1}^2)$ is the area for each equidistant ring.

3. Results

3.1. Scaffolds

Poly(D,L-lactide) macromers were successfully synthesised, the degree of functionalisation of the end groups was more than 95%. After mixing with diluent, photo-initiator and dye, the PDLLA resin was used to build the designed scaffolds by stereolithography. After extraction and drying, the built scaffolds were visualised by μCT imaging. Fig. 1 shows that the scaffold designs were very accurately reproduced. The porosity gradients in the built type G scaffolds can be clearly seen.

For both scaffold types, Fig. 2 shows the distribution of local porosity values as a function of distance from the scaffold central axis. Data from the computer designs as well as from the μCT analyses are presented. The porosity gradient in the type G scaffold leads to a gradient in pore size as well; sizes range from approximately 500 μm in the centre of the scaffold to 250 μm at the periphery.

The type I scaffold shows low variance in porosity and pore size. An overall porosity of 62 ± 1% was determined, with an average pore size of 412 ± 13 μm. For the type I scaffold in particular, the periodicity of the trigonometric functions is reflected by the regular oscillations in the determined local porosity values from the centre of the scaffold outwards. Although in the case of this scaffold type an isotropic porosity of 55% was designed, the μCT data show that the local porosity increases from the centre of the scaffold outwards towards its perimeter. This is the result of overcure, a phenomenon that can occur in the fabrication of porous structures by stereolithography [6]. In the type G scaffold, the effect of overcure is minimal because of the high porosity values in the central region of the scaffold.

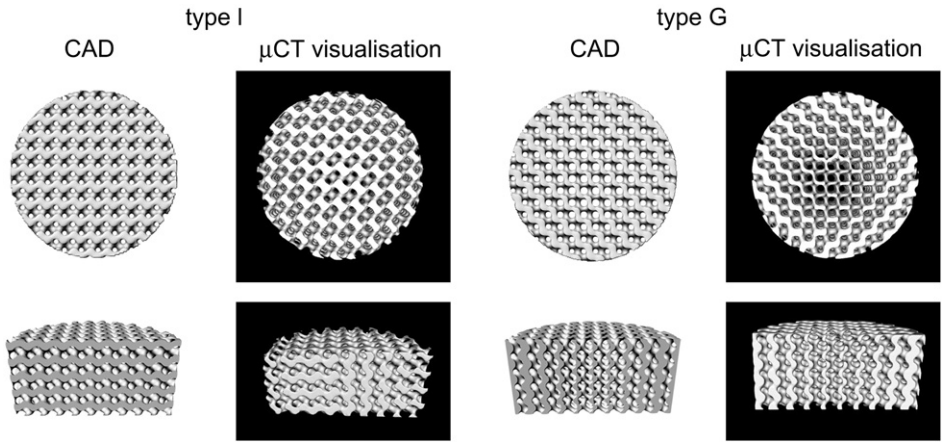

Fig. 1. Top row: top-view images of type I (isotropic design) and type G (gradient design) gyroid scaffolds comparing the computer-aided designs (CAD) with μCT-visualisations of the built structures. Bottom row: cross-sections, clearly showing the gradient in porosity and pore size in the type G scaffold. The diameter of the scaffolds is 8 mm.

3.2. Fluid flow modelling

The flow of fluid through both scaffold architectures was modelled using a computational fluid dynamics approach. To represent the scaffold pore architectures, data from the μCT analyses of the built structures (and not those of the computer designs) were used. The modelling, in which the geometry of the perfusion bioreactor chamber was taken into account as well, resulted in the velocity profiles depicted in Fig. 3. Here, the values of the local fluid velocities are shown as coloured vectors. The characteristic zero mean-curvature of the gyroid pore network architecture implies the absence of flow-disturbing elements. In the given perfusion regime, this results in laminar fluid flows (the maximum calculated Reynolds number is 0.12). Average fluid flow velocities are 0.86 mm/s for both scaffold types. Parabolic fluid velocity profiles develop in each of the channels that run through the scaffolds; the local velocity is highest in the centre of the channel. The modelling shows, that in the type I scaffold the flow profile is quite uniform with maximum velocities of approximately 2.8 mm/s. In the type G scaffold undisturbed laminar flows are also observed, but the radial gradient in porosity leads to a clear gradient in fluid flow velocities. For this scaffold architecture the maximum velocities in the central part of the scaffold are close to 4.0 mm/s, while they strongly decrease to near zero at the periphery. The (direction of the) observed gradient in flow velocities is due to the lower resistance of the larger-diameter channels.

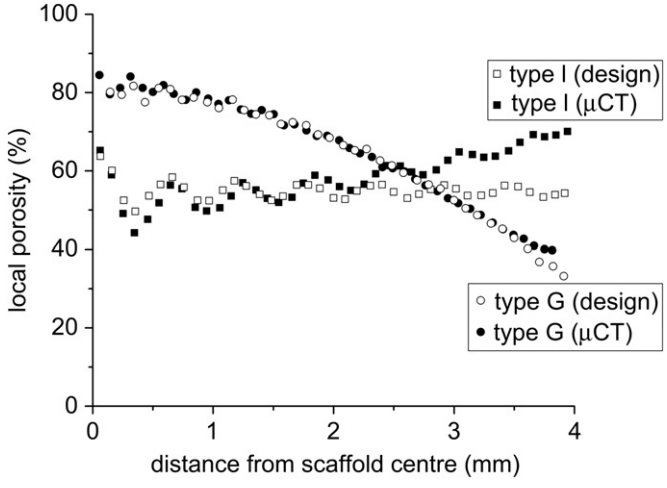

Fig. 2. Local porosity as a function of the distance from the central axis of the scaffold, for cylindrical type I (isotropic) and type G (gradient) scaffolds. The data from the μCT analyses (average of 2 samples each) are compared to the computer-aided designs. Local porosity values are determined at 100 μm intervals.

At the scaffold wall the velocity of the fluid is zero, and wall shear rates are best used to describe the velocity with which suspended cells flow past the surface of the pores. Wall shear rate is defined as the slope of the velocity profile at the fluid–wall interface:. The lower part in Fig. 3 shows 3D views of the scaffolds, where part of the scaffolds is coloured to indicate the distribution of local wall shear rate values. Here, the uniformity of the fluid velocity profile in scaffold type I is also reflected in rather uniform wall shear rates throughout the structure. In contrast, scaffold type G shows considerably reduced wall shear rates towards the periphery of the scaffold when compared to wall shear rates in the centre.

The wall shear rate not only determines the velocity of the passing cell suspension, but it also determines the hydrodynamic force that adhering cells are exposed to. This force can be expressed per unit of area as the wall shear stress (in Pa), and is the product of the wall shear rate and the kinematic viscosity of the fluid medium. The wall shear stress is therefore an important parameter in cell adhesion processes [7]. The average wall shear stresses in scaffold types I and G are 31 and 27 mPa, respectively, and range from near-zero values to maximum local values of approximately 65 mPa. The effects of flow-induced shear stress on cell adhesion have been studied extensively [8,9,10]. The critical shear stress for cell detachment to occur depends on the material on which the cells are cultured, but has been found to range between 1 and 3 Pa [11,12,13]. For the range of wall shear stress values occurring in our perfusion setup, flow-induced cell detachment will not occur.

3.3. Assessment of cell distributions

Upon perfusion seeding, stained constructs were analysed by confocal microscopy. Imaging of the cells and the cell distribution by confocal microscopy and modelling the fluid flow during perfusion cell seeding, allows comparing the spatial density of adhering seeded cell with spatial fluid flow conditions. The example in Fig. 4 shows a cross-section of a type I scaffold (10 μm confocal thickness) where we can distinguish individual cells adhering to the scaffold surface (see insert). The right part of the figure shows the modelled wall shear rate profile in a cross-section. The insert shows that at a small size scale (within a pore), the shear rates range between 0 and 30 s^{-1}. The macroscopic distribution of shear rates, however, is homogeneous; only little differences in shear rate values are observed when comparing unit cells from the central part of the scaffold to those at the periphery.

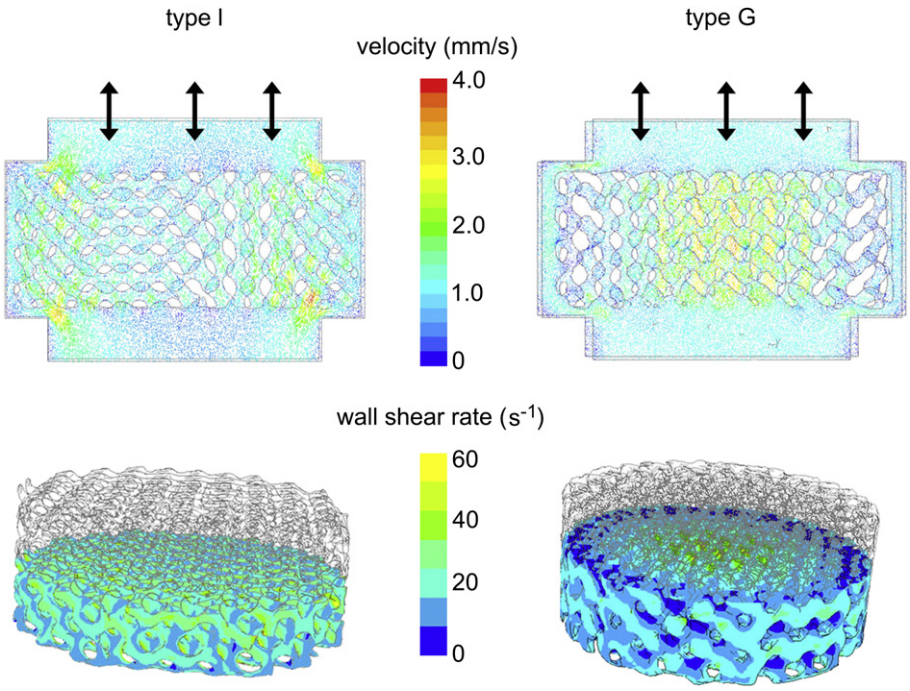

Fig. 3. Fluid flow velocity- and wall shear rate profiles for scaffold types I (isotropic) and G (gradient). The velocity vectors between two parallel sections (at a distance of 0.5 mm) in the direction of the flow path are shown. The diameter of the scaffolds is 8 mm. The spots with high local velocities at the scaffold edges (inlet and outlet) are artefacts.

Fig. 5 depicts thresholded confocal microscopy images of both scaffold types. The cell densities in confocal microscopy images will depend on the surface area available for cell adhesion. For both scaffold types a surface area of $1.2 \cdot 10^3$ mm^2 was determined by μCT, corresponding to an overall specific surface area of 4.8 mm^{-1}. As a result of the well-defined and repetitive nature of the pore network architectures, the local values for the specific surface area (distribution of surface area throughout the scaffold) show only minimal fluctuation. It is therefore possible to compare the observed cell densities in different regions of both scaffold types.

The top left image in Fig. 5 shows a very homogeneous distribution of cells after seeding of the type I scaffold, determined, by inducing uniform velocity- and wall shear rate profiles of the flowing cell suspension. For the type G scaffold, with a radial gradient on pore size and porosity, an anisotropic distribution of cells is observed after perfusion cell seeding. The top right image in Fig. 5 shows that the cell density is markedly higher in the centre of the scaffold than at the periphery.

The distribution of adherent cells was quantified by determining the cell density as a function of the distance in radial direction from the scaffold centre. Fig. 6 depicts the radial distribution of cell densities as histograms, determined from the thresholded images of the cell densities on the different scaffolds such as shown in Fig. 5. Here, the presented values are an average of at least 9 subsets from 3 different scaffolds, each of 70 μm thickness. The values are normalised for each image to enable direct comparison of the relative cell distributions. Besides the radial cell distributions, the corresponding modelled local average wall shear rates are shown.

For the isotropic scaffold (type I), a uniform distribution in the cell density and in the modelled average wall shear rate can be observed. The average wall shear rate values are scattered over a relatively small range of 16–24 s^{-1}, and the values show no relation with location in the scaffold or cell density. The regular isotropic architecture of the scaffold leads to a uniform distribution of flow and results in very homogeneously seeded scaffolds.

In the gradient type G scaffold however, we clearly see anisotropic distributions of seeded cell densities and wall shear rates. Both the cell density and the wall shear rate are high in the centre of the scaffold and much lower at the periphery. The polar moments of inertia give a quantitative measure of how much a radial distribution is spread outwards. For the average wall shear rate the type G scaffold has a value of $6.4.10^3$ s^{-1} whereas the type I scaffold has a value of $8.4.10^3$ s^{-1}. For the relative cell density these values are $3.0.10^2$ and $6.6.10^2$ respectively. As far as the gradient scaffold is concerned, the correlation between the cell density and the modelled average wall shear rate is clearly visualised in the bottom right image of Fig. 6. It is apparent that the highest cell densities in the seeded scaffolds are observed in regions were the wall shear rate of the fluid flow was highest.

4. Discussion

Under flow conditions, the deposition rate of suspended particles on a surface depends on many parameters such as advective transport and diffusivity [14], colloidal interactions [15], concentrations of ligands and receptors [16], binding strengths and bond-forming kinetics [17] and available surface area [18]. Because of the well-defined scaffold architectures and the constant perfusion conditions, many of these parameters do not vary throughout the scaffolds in our perfusion seeding experiments. We can therefore directly assess how flow parameters affect the final distribution of cells upon bioreactor seeding throughout scaffolds with different geometries.

When looking solely at cell–material interactions under fluid flow, it seems contradictory that areas of highest shear and fluid velocity would have higher cell numbers. From this it follows that the relative cell densities resulting from perfusion seeding depend more on the delivery of cells to the different regions of the scaffold than on the kinetics of the cell attachment process that follows, as in the employed shear stress regime no cell detachment can be expected. As in our experiments the flow is laminar, the suspended cells will follow the flow profile (like tracer particles), with minimal advective transport in directions perpendicular to the flow. Only cells close to the pore wall of the scaffold are likely to contact the

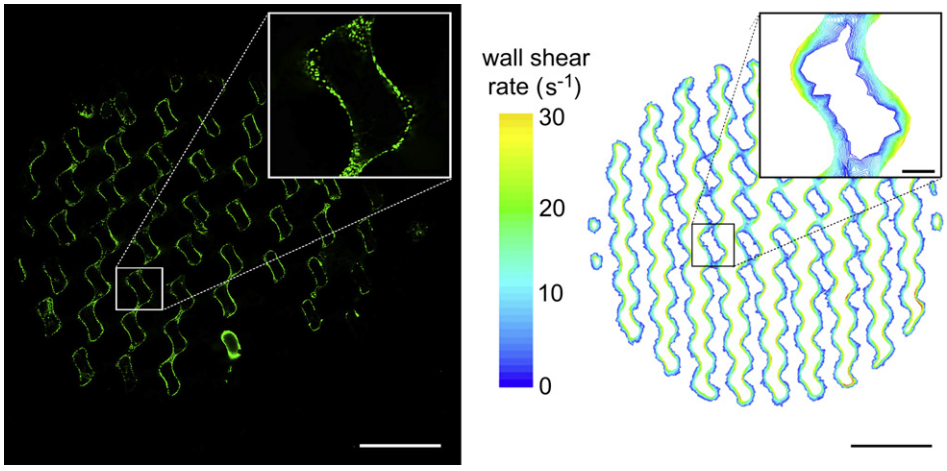

Fig. 4. Left: representative confocal microscopy image of a type I gyroid scaffold seeded with cells, showing the distribution of live adhering cells throughout a cross-section of the scaffold. Right: image of a similar cross-section, showing the modelled distribution wall shear rates of the fluid during perfusion cell seeding. Scale bars are 2 mm for the larger images and 200 μm for the inserts.

surface. As the wall shear rate is a measure of the velocity of the cell suspension close to the scaffold pore wall, it determines the number of cells that flow past the surface per unit of time. This correlation is clearly shown in the right parts of Fig. 6, where the highest cell numbers are close to the centre of the type G scaffold, where wall shear rates are highest.

From this, it follows that we can influence distributions of seeded cells in perfusion seeding by tailoring the architecture of the pore network of the scaffold. In well-defined isotropic gyroid architectures we can obtain very homogeneous distributions of adhering cells, while gradients in pore size and porosity lead to gradients in cell densities. The scaffold architecture affects the local fluid flow velocities of the cell suspension, the number of cell-scaffold contacts per time unit and, therefore, the local cell deposition rates. By preparing other scaffolds with designed architectures, other flow profiles and other cell distributions in the scaffolds may be obtained. Other cell

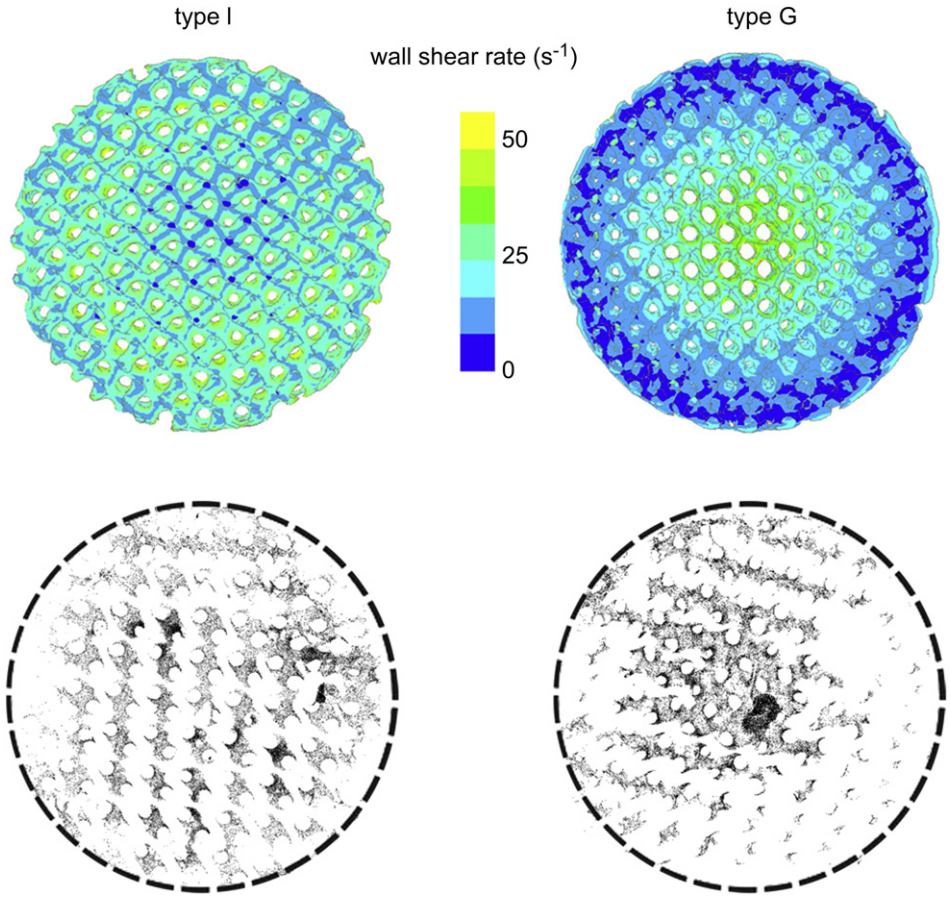

Fig. 5. Comparison of the distribution of cell densities and wall shear rates in cross-sections of type I (isotropic) and type G (gradient) scaffolds. Top: representative thresholded z-stacks of confocal microscopy images (500 μm thickness) showing adhering cells after perfusion seeding. Bottom: middle cross-sections of scaffolds showing wall shear rate distributions of the fluid during perfusion cell seeding.

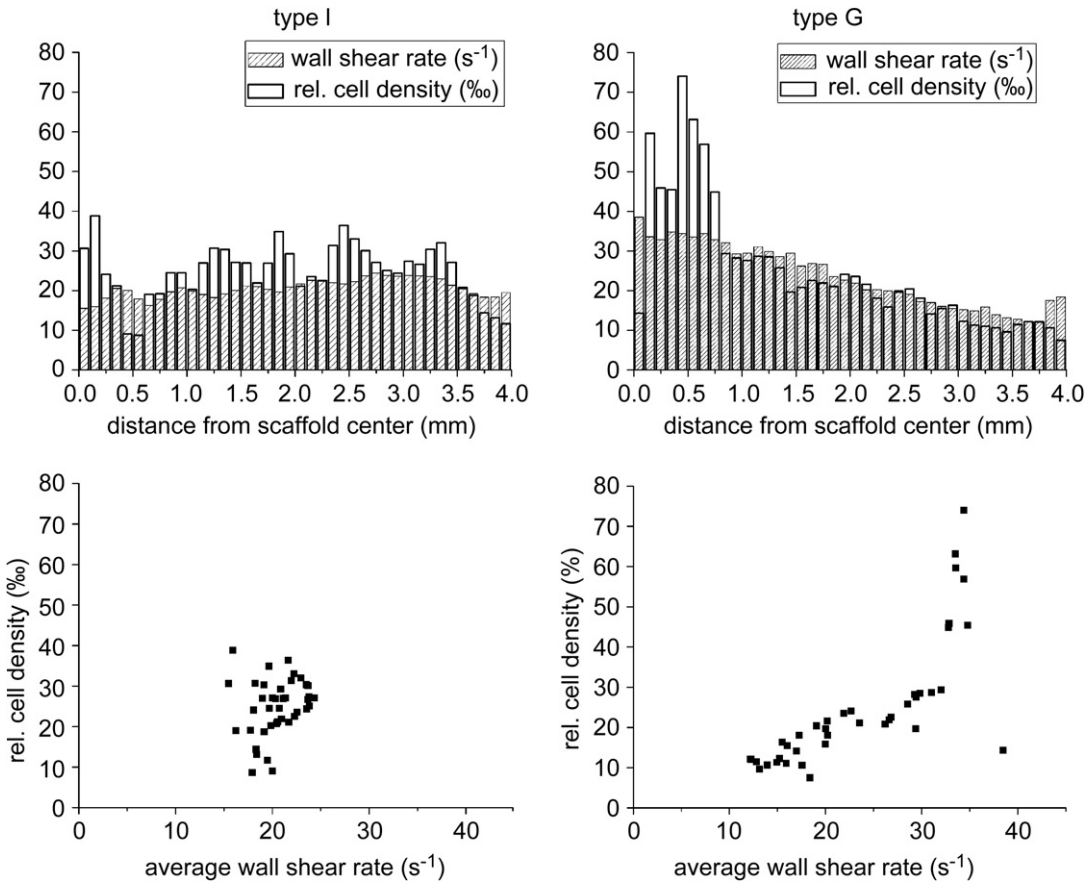

Fig. 6. Quantitative comparison of the distributions in modelled wall shear rate and measured cell density in cross-sections of the isotropic type I (left) and gradient type G (right) scaffolds. Top: distributions of local average wall shear rates (s^{-1}) and of cell densities as a function of the distance in the radial direction from the scaffold centre. Bottom: scatter plot of the cell density as a function of the modelled local average wall shear rate.

types may exhibit different seeding kinetics as these may have different types and densities of adhesion molecules. However, since the flow-induced transportation of cells towards the scaffold pore surface seems to be the determining factor in our setup, similar cell distributions may be expected using different cells and/or scaffold materials. Under the well-controlled conditions in the used perfusion bioreactor system —applying wall shear stresses that are well below values typical for cell detachment to occur- the internal scaffold pore architecture is the determining factor influencing the final cell distribution.

As we have studied only one time-point, the specific kinetics of the cell seeding process can not be derived from our data. For this, cell adhesion experiments using a flow displacement system should be performed as a function of time [19]. Shear rate-dependent adsorption rates can be determined in such experiments. The effect of the three-dimensional architecture of the porous structure could then be investigated separately, and better understanding and control of regional differences in cell deposition could be achieved. Furthermore, critical wall shear stress values could be determined at higher flow rates.

In this work we related averaged cell densities to averaged wall shear rates, as a function of distance from the scaffold central axis. A next step in the development of this model system would be to assess cell distributions at the pore level, since in each pore a range of wall shear rates exists. Such a model system would then enable to experimentally validate theories of mechano-regulation of cell behaviour. These theories are based on computational models, in which the probabilistic behaviour of cells resulting from mechanical stimuli acting at the cellular level is modelled. In this way, cell proliferation and differentiation and extracellular matrix formation could be predicted [20,21]. Particularly the ability to visualise individual cells and compute their local hydrodynamic environment provides an experimental framework to test, adjust and support these theories.

5. Conclusions

We have developed a model system to assess the influence of local fluid flow characteristics in designed porous scaffolding structures on the distribution of cells upon perfusion seeding. The density of adhering cells was correlated to the local average wall shear rate at the surface of the pore walls. While scaffolds with an isotropic gyroid pore network architecture show very homogeneous distributions of shear rates and cell seeding densities upon perfusion cell seeding, gyroid scaffolds prepared with gradients in pore size and porosity show anisotropic adherent cell densities. The highest cell densities in the scaffolds could be related to regions with larger pores, higher fluid flow velocities and higher wall shear rates. The ability to influence the distribution of seeded cells in a porous structure upon seeding will be fundamental to control the engineering of complex three-dimensional tissue constructs with defined structural organisations.

Acknowledgements

We acknowledge the European Union for their financial support (STEPS project, FP6-500465).

Appendix

Figures with essential colour discrimination. Certain figures in this article, particularly Figs. 3, 4, and 5, are difficult to interpret in black and white. The full colour images can be found in the on-line version, at doi:10.1016/j.biomaterials.2011.01.023.

References

[1] Marsano A, Wendt D, Raiteri R, Gottardi R, Stolz M, Wirz D, et al. Use of hydrodynamic forces to engineer cartilaginous tissues resembling the non-uniform structure and function of meniscus. Biomaterials 2006;27(35):5927–34.
[2] Cioffi M, Kuffer J, Strobel S, Dubini G, Martin I, Wendt D. Computational evaluation of oxygen and shear stress distributions in 3D perfusion culture systems: macro-scale and micro-structured models. J Biomech 2008;41(14):2918–25.
[3] Melchels FPW, Bertoldi K, Gabbrielli R, Velders AH, Feijen J, Grijpma DW. Mathematically defined tissue engineering scaffold architectures prepared by stereolithography. Biomaterials 2010;31:6909–16.
[4] Wendt D, Marsano A, Jakob M, Heberer M, Martin I. Oscillating perfusion of cell suspensions through three-dimensional scaffolds enhances cell seeding efficiency and uniformity. Biotechnol Bioeng 2003;84(2):205–14.
[5] Wendt D, Stroebel S, Jakob M, John GT, Martin I. Uniform tissues engineered by seeding and culturing cells in 3D scaffolds under perfusion at defined oxygen tensions. Biorheology 2006;43(3–4):481–8.
[6] Melchels FPW, Feijen J, Grijpma DW. A poly(D, L-lactide) resin for the preparation of tissue engineering scaffolds by stereolithography. Biomaterials 2009;30(23–24):3801–9.
[7] Morigi M, Zoja C, Figliuzzi M, Foppolo M, Micheletti G, Bontempelli M, et al. Fluid shear-stress modulates surface expression of adhesion molecules by endothelial-cells. Blood 1995;85(7):1696–703.
[8] Ando J, Yamamoto K. Vascular mechanobiology - endothelial cell responses to fluid shear stress. Circ J 2009;73(11):1983–92.
[9] Rosenman JE, Kempczinski RF, Pearce WH, Silberstein EB. Kinetics of endothelial-cell seeding. J Vasc Surg 1985;2(6):778–84.
[10] Feugier P, Black RA, Hunt JA, How TV. Attachment, morphology and adherence of human endothelial cells to vascular prosthesis materials under the action of shear stress. Biomaterials 2005;26(13):1457–66.
[11] Isenberg BC, Williams C, Tranquillo RT. Endothelialization and flow conditioning of fibrin-based media-equivalents. Ann Biomed Eng 2006;34(6):971–85.
[12] Macario DK, Entersz I, Abboud JP, Nackman GB. Inhibition of apoptosis prevents shear-induced detachment of endothelial cells. J Surg Res 2008;147(2):282–9.
[13] Smith RL, Donlon BS, Gupta MK, Mohtai M, Das P, Carter DR, et al. Effects of fluid-induced shear on articular chondrocyte morphology and metabolism in vitro. J Orthop Res 1995;13(6):824–31.
[14] Adamczyk Z, Vandeven TGM. Deposition of particles under external forces in laminar-flow through parallel-plate and cylindrical channels. J Colloid Interf Sci 1981;80(2):340–56.
[15] Sjollema J, Busscher HJ. Deposition of polystyrene latex-particles toward polymethylmethacrylate in a parallel plate flow cell. J Colloid Interf Sci 1989;132(2):382–94.
[16] Cozensroberts C, Quinn JA, Lauffenburger DA. Receptor-mediated adhesion phenomena - model studies with the radial-flow detachment assay. Biophys J 1990;58(1):107–25.
[17] Hammer DA, Lauffenburger DA. A dynamic-model for receptor-mediated cell-adhesion to surfaces. Biophys J 1987;52(3):475–87.
[18] Meinders JM, Busscher HJ. Adsorption and desorption of colloidal particles on glass in a parallel-plate flow chamber - influence of ionic-strength and shear rate. Colloid Polym Sci 1994;272(4):478–86.
[19] Busscher HJ, van der Mei HC. Microbial adhesion in flow displacement systems. Clin Microbiol Rev 2006;19(1):127–41.
[20] Sandino C, Checa S, Prendergast PJ, Lacroix D. Simulation of angiogenesis and cell differentiation in a CaP scaffold subjected to compressive strains using a lattice modeling approach. Biomaterials 2010;31(8):2446–52.
[21] Olivares AL, Marshal E, Planell JA, Lacroix D. Finite element study of scaffold architecture design and culture conditions for tissue engineering. Biomaterials 2009;30(30):6142–9.